

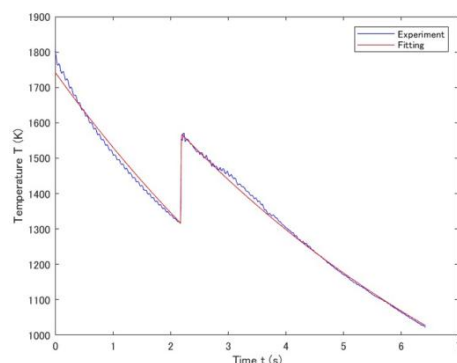
PS17

無容器溶融法による酸化物過冷却凝固時の核形成解析

Analysis of nucleation during supercooled solidification
of oxides using the containerless suspension method佐久間康¹, 崎山英治¹, 渡邊匡人²Yasushi SAKUMA¹, Eizi SAKIYAMA¹ and Masahito WATABABE²¹ 学習院大学自然科学研究科, Graduate School of Science, Gakushuin University, Tokyo, Japan² 学習院大学理学部, Faculty of Science, Gakushuin University Faculty of Science, Tokyo, Japan

* Correspondence: 25141004@gakushuin.ac.jp

Abstract: Solidification from supercooling has been studied extensively from the perspectives of crystal growth and nucleation. Until now, many studies have applied heat transfer equations to continuous cooling curves, but they have been unable to describe the entire cooling curve of solidification, including recrystallization (radiation during the release of latent heat of solidification) in cases of large supercooling. Therefore, in addition to the heat transfer equation, a method was proposed that incorporates the JMAK equation, which adds the solidification fraction to the recrystallization process, to describe the entire solidification cooling curve¹⁾. This method enables the description of the cooling curve even in cases of large supercooling and provides information on nucleation. In this study, solidification experiments of FeO-TiO₂ were conducted using a gas jet suspension apparatus, and the overall supercooling curve of solidification was obtained. The supercooling curve was fitted with a model equation using the heat transport equation and the JMAK equation. By calculating the classical nucleation frequency from the fitting parameters, it was demonstrated that oxides are less prone to nucleation than alloys. This study is significant for understanding nucleation in oxides.

**Keywords:** Supercooled melt, Aerodynamic levitation, interfacial free energy, FeTiO₃, recrystallization

1. Introduction

Research and development on the in-situ utilization of lunar resources has progressed in recent years. Concepts such as processing lunar regolith to construct structures and extracting metallic resources have been proposed. To realize these concepts, it is essential to understand the characteristics of lunar regolith under the ultra-high vacuum and low-gravity environment of the lunar surface and to design appropriate processes. Additionally, it is known that localized strong magnetic fields exist on the lunar surface. This magnetic anomaly is presumed to result from the rapid cooling and solidification of high-temperature melted regolith following meteorite impacts, leading to the precipitation of metallic iron in regions with high Fe content. Efficient extraction of Fe in these areas is anticipated for future lunar regolith utilization. Therefore, we simulated the rapid cooling and solidification process from a high-temperature liquid state caused by meteorite impacts using the aerodynamic levitation method, synthesized FeO-TiO₂ powder into FeTiO₃

(ilmenite), and observed the formation of a continuous solid solution of FeTiO_3 (ilmenite) and Fe_3O_4 (magnetite) based on their magnetic properties. At $\text{FeO}:\text{TiO}_2 = 50:50$ at%, which corresponds to the stoichiometric composition of ilmenite, the equilibrium phase diagram indicates that ilmenite should form as a single phase. However, in the aerodynamic levitation method, solid solutions of ilmenite and magnetite were obtained during solidification from a supercooled state.

From these backgrounds, we investigated the nucleation process of crystal growth from an $\text{FeO}:\text{TiO}_2 = 50:50$ at% undercooled melt and examined the mechanism of solid solution formation. Heat transfer equations to continuous cooling curves²⁾, and the cooling curve for the entire solidification process, including the recalescence (radiation during latent heat release) phenomenon from large supercooling, could not be described. In previous studies, solidification from supercooling was often described by applying the classical Johnson–Mehl–Avrami–Kolmogorov (JMAK) equation, the transformed fraction upon dendritic solidification was described approximately. The JMAK equation was only adopted to describe the subject to small undercooling, but the corresponding works after large undercooling have rarely been reported owing to the complicated reaction mechanism. Recently, an analytical approach combining the heat flow equation and the JMAK equation was proposed to describe the thermal history of supercooled liquid including the primary solidification. The model equation incorporating a function simulating the temperature jump during recalescence into the solidification rate change term was proposed, enabling the reproduction of the cooling curve for crystallization from undercooling¹⁾. In this study, we applied this model equation to the crystallization of a supercooled melt of $\text{FeO}:\text{TiO}_2 = 50:50$ at% and derived a nucleation frequency parameter to elucidate the mechanism of solid solution formation between FeTiO_3 and Fe_3O_4 .

2. Experiments and equations

2.1 gas flotation experiment

2.1.1 About the sample

The sample used was $\text{FeO}-\text{TiO}_2$ (mol% 1:1). Since it is difficult to float the sample using the gas flotation method when it is in powder form, it must be a solid of a certain size. Therefore, sintering was first performed using a laser. Sintering is the process of solidifying powdered metal at a temperature lower than its melting point. These samples were placed on a sintering table and irradiated with a CO_2 laser. The sintered samples yielded the results shown in **Fig.1**. This is a photograph of the burnt area where the laser was applied. It was found that when the laser was applied, a cylindrical hole was formed, and it did not become spherical.

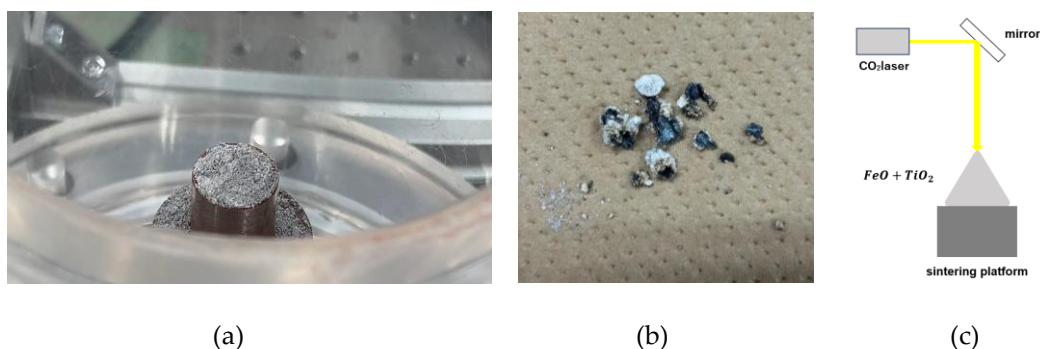


Figure 1. $\text{FeO}-\text{TiO}_2$ sample charring. (a) Sample placed on sintering platform, (b) Part of the sample hit by the laser, (c) Experimental diagram.

Since the objective here was not to form spheres but to solidify the material, gas flotation experiments were conducted using the solidified samples. However, various issues were identified.

- Recalculation does not occur when the sample is small.

- The sample is damaged when it is collected

The reason for the breakage is thought to be that the sample did not melt completely, preventing it from solidifying uniformly inside the sample. (**Fig.2**)

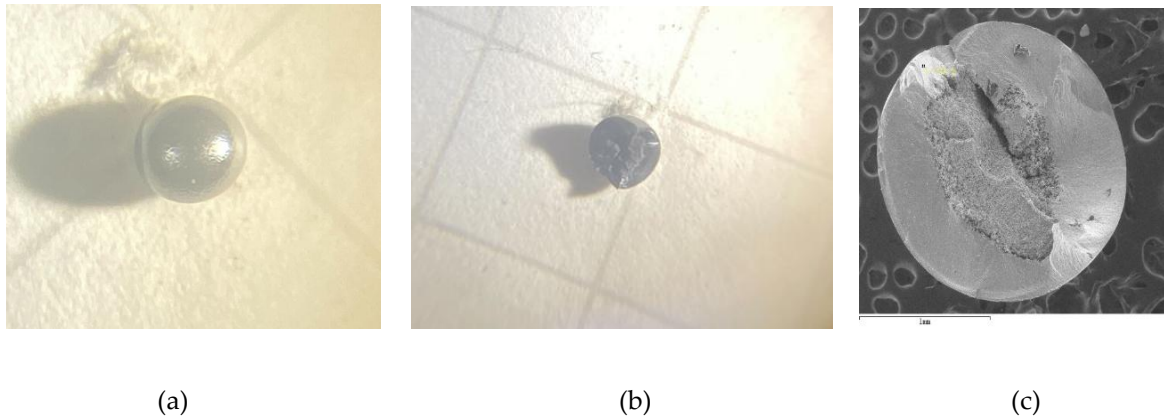


Figure 2. Melted FeO-TiO₂ sample (a) sphere, (b) fragment ,(c)Cross section of damaged sample photographed with SEM.

Since the uniformity of the powdered sample, which resembled charcoal, was questionable, a press machine was used to compact the sample in order to make the powder uniform. Using this sample (**Fig.3**) made it uniform and resolved issues with measuring recaleness and recovering the sample. Therefore, we used this method for measurement from the middle of the experiment. However, measurement is not always possible, and there are many things that cannot be known without conducting gas flotation experiments.



Figure 3. Powdered sample stirred, pressed, and crushed to a size that can float.

2.1.2 About the experiment

The gas jet flotation method allows samples to float by releasing gas upward and balancing their weight (**Fig.4(a)**). This enables laser irradiation and melting at high temperatures. The procedure is shown below.

1. The sample is suspended in the air atmosphere using Ar gas. The gas is regulated using a variable area flow meter. The sample is observed by shining a backlight laser on it.
2. Melt the sample with a CO₂ laser. Be careful to melt the entire sample. Adjust the gas flow with a variable area flow meter to maintain suspension, and increase the laser output to melt the sample.
3. Stop the laser once melting has occurred. Begin cooling immediately, and by observing the graph of temperature change over time, you can obtain the cooling curve for the entire solidification process, including recrystallization due to supercooling.

4. Combine the obtained cooling curve, heat transfer equation, and JMAK equation model equation to obtain the oxide parameters.

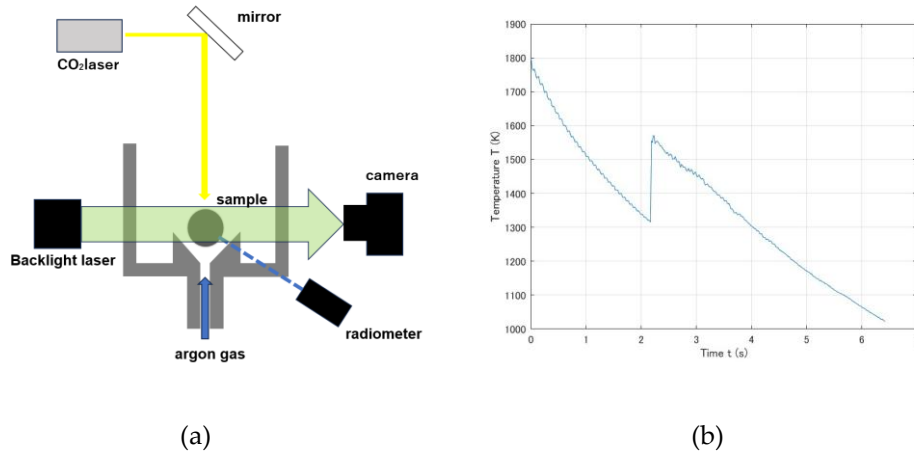


Figure 4. (a) Gas flotation device setup, (b) Graph showing cooling curves obtained from experiments.

2.2 Equations

A model combining the heat transport equation and the JMAK equation (abbreviation for JMAK) has been proposed¹⁾.

$$T = \Phi(t) + \theta f(t), \quad (1)$$

$$\Phi = A \exp(-Bt) + T_G, \quad (2)$$

$$f = 1 - \exp[-k(t - t_n)^3 \xi(t - t_n)], \quad (3)$$

$$\xi(\Delta\tau) = \exp\left[-\frac{1}{a(\pi)^{\frac{1}{2}}} \exp\left(\frac{-\Delta\tau}{a}\right)\right] = \begin{cases} 0 & (\Delta\tau < 0) \\ 1 & (\Delta\tau > 0) \end{cases}, \quad (4)$$

Where T is temperature, θ is supercooling, f is the JMAK equation, A is the difference between the initial temperature T_0 and the ambient temperature T_G , B is $\frac{3h}{\rho cr}$, k is the velocity constant, t is the time at which latent heat release ends, t_n is the time at which latent heat release begins, $t - t_n = \Delta\tau$ is supercooling, and a is a constant. Here, these processes were set in order to apply the JMAK equation to the non-isothermal solidification process.

- (i) isothermal transformation and hard impinge ment (due to random nuclei dispersion) are assumed, where the solid fraction depends only upon time
- (ii) since the cooling curve is measured by infrared pyrometer (focusing on the surface), a surface limited nucleation and a two-dimensional growth can be assumed
- (iii) both the nucleation rate and the growth rate are constant
- (iv) once nucleated, the positions of the grains remain fixed (the role of fluid flow is ignored)
- (v) both dendritic and eutectic grains are assumed to be equiaxed and enveloped within a sphere
- (vi) coalescence and dissolution of the growing grains are ignored.

By using this equation, it became possible to describe the cooling curve of the entire solidification process, including recrystallization due to supercooling. **Figure 5** shows the results of experiments conducted using Ni-B alloys and fitted using the model equation¹⁾.

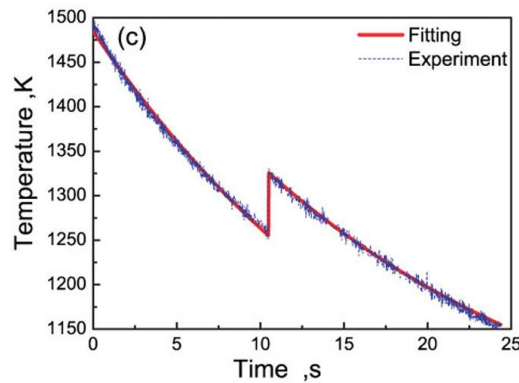


Figure 5. Cooling curves upon undercooled solidification of Ni-B alloy subjected to undercoolings.

2.3 How to fit the cooling curve obtained in the experiment to the model equation

Plot a graph using the values obtained from the experiment and the values obtained from the fitting. To do this, solve the model equation. The procedure is shown below.

1. Fit the cooling curve using Eq. (5) and obtain a single optimal solution for k . Substitute T_N , θ and t_n obtained from the experiment. Vary T and t and obtain a single optimal solution for k .
 2. The entire cooling curve is fitted using the obtained k value, and A , B , and T_G are determined by Eq.(6).
- This allows you to draw graphs (**Fig.6**).
3. Perform fitting of the cooling curve obtained in the experiment and the model equation (**Fig.7**).
 4. If they overlap, use the parameters for calculation.

$$T = T_N + \theta [1 - \exp[-k(t - t_n)^3 \xi(t - t_n)]], \quad (5)$$

$$T = A \exp(-Bt) + T_G + \theta [1 - \exp[-k(t - t_n)^3 \xi(t - t_n)]], \quad (6)$$

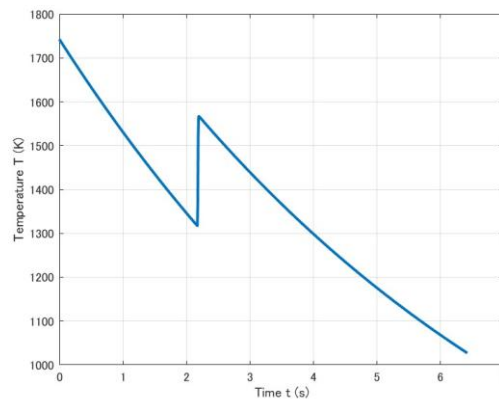


Figure 6. Cooling curve based on model formula

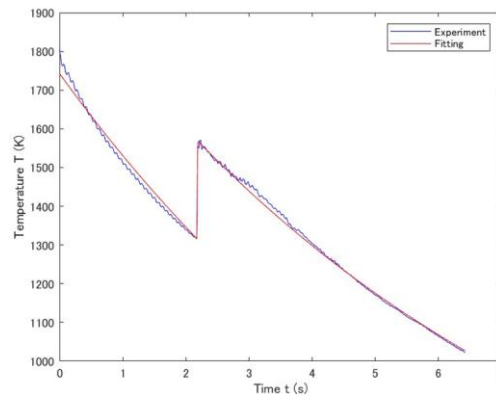


Figure 7. Graph showing the cooling curve obtained in the experiment and the model equation fitting.

3. Result

3.1 Calculation of interfacial free energy

The nuclear production frequency is calculated using the values obtained from the fitting. The formula used is

$$k = \frac{\pi}{3} I_s V^2, \quad (7)$$

θ is the temperature difference during recrystallization, V is the growth rate, k is the rate constant, B is an indicator of heat transfer, and I_s is the nucleation frequency. The results are shown in **Table 1**.

Table 1. Required nuclear production frequency

Values obtained from experiments		Values obtained from fitting		
θ/K	V/ms^{-1}	k	B	$I_s/m^{-2}s^{-1}$
232.2	0.13089	1305212	0.12231	7.3×10^7
238.6	0.14185	2684838	0.12805	1.2×10^8
239.1	0.15648	1513861	0.11094	5.9×10^7

Calculate the interfacial free energy from the nucleation frequency. The nucleation frequency is expressed as follows.

$$I_s \propto \exp \left[\frac{\sigma^3}{k_B T \Delta G} \right], \quad (8)$$

σ is the interfacial free energy, ΔG is the critical nucleation energy, k_B is the Boltzmann constant, and T is the melting point. The results of calculating the interfacial free energy are as follows.

Table 2. Comparison of interfacial free energy between Ni-B alloys and oxides

oxide($FeTiO_3$)	alloy($Ni_{86}B_{14}$)	oxide($FeTiO_3$)	alloy($Ni_{86}B_{14}$)
$I_s/m^{-2}s^{-1}$	$I_s/m^{-2}s^{-1}$	σ/Jm^{-2}	σ/Jm^{-2}
7.3×10^7	8.7×10^4	7.28×10^{-7}	5.98×10^{-7}
1.2×10^8	1.0×10^5	7.37×10^{-7}	5.99×10^{-7}
5.9×10^7	8.2×10^5	7.26×10^{-7}	6.29×10^{-7}

Compared to alloys, oxide samples have higher interface free energy. This indicates that oxides are less likely to form nuclei. This result is consistent with the explanation of oxides.

4. Conclusion

In this study, experiments were conducted to obtain cooling curves of oxides during supercooling using a gas flotation apparatus. It was confirmed that experiments similar to those conducted on alloys could also be performed on oxides. In addition, an investigation of nucleation was conducted by fitting the cooling curves using a model equation. The model equation used a method that describes the overall cooling curve of solidification by adding the solidification fraction to the JMAK equation, which is a recursion equation, in addition to the heat transfer equation¹⁾. The results obtained from the fitting were evaluated in terms of nucleation in $FeTiO_3$ compared to Ni-B alloys. The interfacial free energy was evaluated as $7.30 \times 10^{-7} Jm^{-2}$ for Ni-B alloys and $6.09 \times 10^{-7} Jm^{-2}$ for $FeTiO_3$. These results are consistent with the property of oxides being less prone to nucleation. Further insights are expected to be gained through continued gas suspension experiments and model fitting.

Conflicts of Interest

The authors state no conflict of interest.

Nomenclature

T	Temperature (K)
θ	Supercooling (K)
A	Difference between the initial temperature T_0 and the ambient temperature T_G (K)
B	Thermal relaxation rate(s^{-1})
ρ	Density(kg/m^3)
c	Specific heat($J/(kg \cdot K)$)
r	Radius(m)
h	Heat transfer coefficient($W/(m^2 \cdot K)$)
k	Velocity constant (N.D.)
t	Time at which latent heat release ends (s)
t_n	Time at which latent heat release begins (s)
a	A constant(N.D.)
T_G	Ambient temperature(K)
f	Solid fraction(N.D.)
T_N	Initial temperature of recarbonization(K)
V	Growth rate(ms^{-1})

I_s	Nucleation Rate($\text{m}^{-2}\text{s}^{-1}$)
σ	Interfacial Free Energy(Jm^{-2})
ΔG	Critical nucleation energy Energy(J)
k_B	Boltzmann Constant(J/K)

References

- 1) J. F. Xu, F. Liu*, K. Zhang and M. M. Gong: Simple approach for description of undercooled solidification, Mater. Sci. Technol, **28** (2012) 274, DOI: [10.1179/1743284711Y.00000000030](https://doi.org/10.1179/1743284711Y.00000000030).
- 2) W. Yang, F. Liu , H. Liu, H.F. Wang, G.C. Yang and Y.H. Zhou: Numerical description for the recalescence of bulk-undercooled Cu70Ni30 alloy, J. Cryst. Growth, **311** (2009) 3225, DOI: [10.1016/j.jcrysgro.2009.03.030](https://doi.org/10.1016/j.jcrysgro.2009.03.030)



© 2025 by the authors. Submitted for possible open access publication under the terms and conditions of the Creative Commons Attribution (CC BY) license (<http://creativecommons.org/licenses/by/4.0/>).